Contents lists available atGrowingScience

Engineering Solid Mechanics

homepage: www.GrowingScience.com/esm

Using finite element modeling to predict stress concentration factors in tubular T, Y and K joints

Abdelhak Berkia[a*], Billel Rebai[b*], Khelifa Mansouri[a,c], Mourad Chitour[a] and Faicel Khadraoui[a]

[a]*Department of Mechanic Engineering, Abbes Laghrour University, Khenchela, 40000, Algeria*
[b]*Department of Civil Engineering, Abbes Laghrour University, Khenchela, 40000, Algeria*
[c]*Engineering and Advanced Materials Science Laboratory (ISMA), Abbes Laghrour University, Khenchela, Algeria*

A R T I C L E I N F O

Article history:
Received 17 August 2023
Accepted 6 November 2023
Available online
6 November 2023

Keywords:
Steel pipe
Welding
Tensile
Bending
Tubular junctions
Finite element

A B S T R A C T

Tubular offshore structures are commonly assembled using welded joints, creating areas of stress concentration and potential fatigue failure. This study focuses on tubular T, Y and K joints, a common offshore structural component. Finite element modeling is used to predict stress concentration factors (K_t) for various loading conditions on the T, Y and K joints. The goal is to calculate K_t values and compare them to existing theoretical solutions from literature. Additionally, the influence of different loading modes (tension, bending) on the K_t values is investigated. By using advanced modeling techniques, this work aims to provide new insight into the behavior of tubular T, Y and K joints connections under realistic offshore loading conditions. The results can help improve design standards and fatigue life predictions for these critical structural joints.

1. Introduction

Tubes are a crucial semi-finished product in steel production (V.A. M Steel Statistical Yearbook 2017). When analyzing structures under repeated loads, existing methods consider the impact of stress concentration on the development of fatigue phenomena (Jukić et al., 2021). However, in tubular assemblies, geometric discontinuities arise due to construction requirements, leading to stress concentrations, particularly near weld beads. These zones pose the risk of initiating and propagating fatigue cracks (Alaoui, 2015). Various researchers have explored stress intensity factors and crack analysis in different contexts (Zhen et al., 2016). Wang and Lambert (2003) employed the weight function method to calculate stress intensity factors for surface cracks in T-plate joints under arbitrary mode I loads. Mansouri et al. (2022) identified distinct microstructures in steel pipe welded joints. El Fakkoussi et al. (2019) utilized finite element methods to compute stress intensity factor K_t in mode I for a longitudinal semi-elliptic crack on the outer surface of a tube. Krešimir et al. (2021) studied thermo-mechanical simulation of welding processes, stress mapping, and stress intensity factor (K_t) calculation. Yao et al. (2023) explored the effects of various influencing factors on stress intensity factors along the crack front, considering crack closure and different conditions under internal pressure. Wang (2016) applied fracture mechanics principles to quantitatively analyze propagating cracks, solving the crack problem in T-shaped welded tees in waste heat boilers. Fustar et al. (2018) presented a review of common fatigue assessment methods used for welded steel joints. OH et al. (2012) estimated stress intensity factors for circumferential cracked pipes under welding residual stress fields.

The primary goal of this study is to calculate stress concentration factors *Kt* in T, Y and K shaped tubular joints and compare them with existing theoretical solutions in the literature. Furthermore, the research aims to investigate the influence of loading modes (tension, bending) on K_t values. By examining these factors, the study seeks to gain valuable insights into the behavior and structural integrity of tubular joints, particularly in the three shaped configurations, which can aid in optimizing their design and performance.

* Corresponding author.
E-mail addresses: berkia.abdelhak@univ-khenchela.dz (A. Berkia) billel.rebai@univ-khenchela.dz (B. Rebai)

ISSN 2291-8752 (Online) - ISSN 2291-8744 (Print)

doi: 10.5267/j.esm.2023.11.002

2. Measurement process

2.1 Parametric formulas

These formulas have been determined on the basis of a large number of analyzes carried out by finite elements and verified by tests on complete models. They are based on the work of several research teams spread over several years (Efthymiou, M. 1988). Beale and Toprac (British Standard 1998) presented a set of parametric equations for T-nodes with axial loading. A numerical investigation of the K_t of T, Y and K nodes has been reported by Reber (Guidance on Design 1995) as part of an extensive program concerning the study of the limit load of tubular nodes. A numerical methodology was employed, based on an analytical solution of the cylindrical shells, following the equations of Donnell (S. A. KARAMANOSet al. 2000) is reported by the parametric formulas.

A numerical technique was employed by Visser (Potvin et al., 1977) to derive the parametric equations for the stress concentrations in the T nodes, using shell-like finite elements, developed by Johnson and Clough (Johnson & Clough, 1968) for the analysis of thin shells. No particular weld modeling was used. Analytical calculations are used less and less directly; these calculations can be done directly using software. Two options are available to the designer:

- The first consists of using numerical calculation tools such as the finite element method to find a numerical K_t value and then perform the classic fatigue calculation.
- The second is a global approach for calculating the fatigue life map, including parameters such as stress concentration and multiaxial stresses (British Standard 1998).

2.2 Applied load

For the study of tubular structures, loads which must be applied to each spacer and which are considered in the calculation of the nodes are represented as follows:

- Axial force (traction Tr),
- In-plane bending (BIP),
- Bending out of plane (BOP).

The other components (transverse shear and torsion moment) are usually neglected since these loads do not induce bending in the skin of the chord. Axial tension, in-plane bending and out-of-plane bending are normally the design criteria for tubular nodes (Efthymiou, 1988).

2.3 Stress distribution

In any mechanical body with discontinuities, the stresses are not uniform along the surface connecting the spacer to the chord (Smedley & Fischer, 1991); Fig. 1 shows the stress distribution in a tubular node with discontinuities in and near the junction (brace chord) (Efthymiou, 1988).

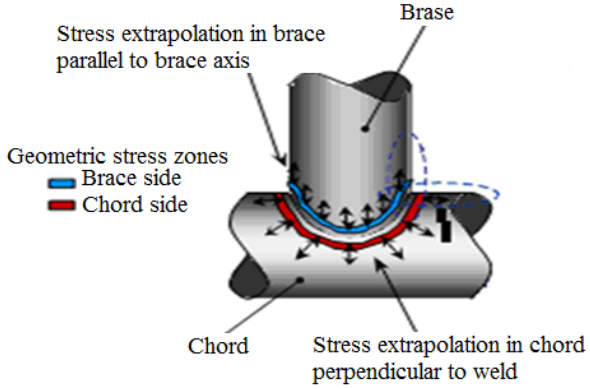

Fig. 1. Stress distribution in a tubular knot (Veritas, 2004).

The stress concentration factor K_t is defined as the ratio of the maximum geometric stress to the nominal stress. The geometric stress σ_{max} includes all stress components in the vicinity of a weld bead, except the nonlinear stress component, which is due to the presence of the weld itself.

3. Numerical simulation

The simulation software used in this study CASTEM software (Castem software). Fig.2 describes the geometry of the structure studied according to (Guidance on Design 1995).

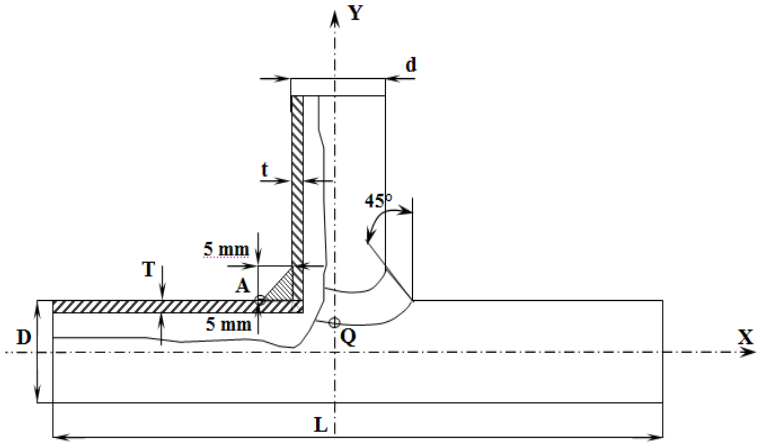

Fig. 2. T Structure.

The weld bead is divided into n identical finite elements around the z axis. In the same way the angle $\Phi = 360°$ all around the closed weld bead is divided by the same number of elements n in order to obtain the angular Φ_1 position of the first element. Consequently, each element i of the weld bead is identified by its angle of positioning Φ_i around the axis z. $\Phi_1 = 360/n$ and $\Phi_{i+1} = \Phi_i + \Phi_1$ (with $1 \le i \le n-1$).

Given the symmetry of the structure (Fig. 3), our study will relate only to the elements located between the pommel point ($\Phi_i = 0$) and the quarter point ($\Phi_i = 90$).

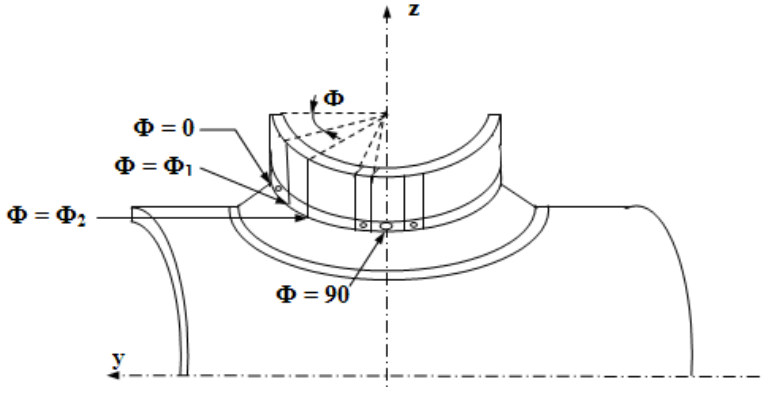

Fig. 3. Positioning angle Φ_i .

The dimensions used in the analysis are reported in Table 1.

The studied structure is made of ordinary steel with the following characteristics:
E=207GPa, ν =0.3, ρ=$7.8E^{-6}Kg/mm^3$ and α=$1.2E^{-5}$ (Guidance on Design 1995). For conditions of limits: Blocking of all translations (U_x, U_y and U_z) and rotations along the X and Y axes (R_x and R_y). The structure is stressed in tension along the ascending Z axis (Fig. 4(a)), along X in bending in the plane (Figure 4(b)) and in bending out of the plane along Y (Fig. 4(c)), with an intensity of ***4 MPa*** for each load. Fig. 5 and Fig. 6 represent the conditions of limits for Y and K structures.

Table 1. Structure dimensions (Guidance on Design 1995).

L = 4130mm	*T = 12.7mm*
d = 406mm	*D = 508mm*
t = 9.5mm	*Weld : 5mm x 5mm*
d/D = 0.8	*R/T = 20*
t/T = 0.75	*L/D = 16.25*
L = 4130mm	*T = 12.7mm*

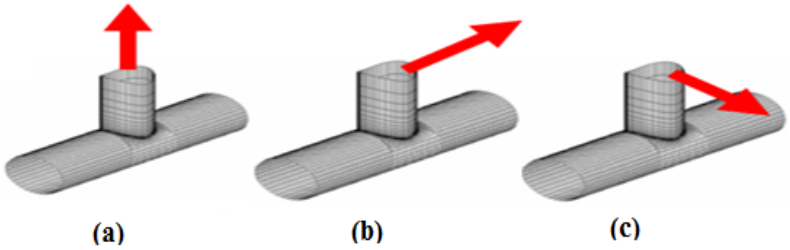

Fig. 4. Loads applied to T structure.

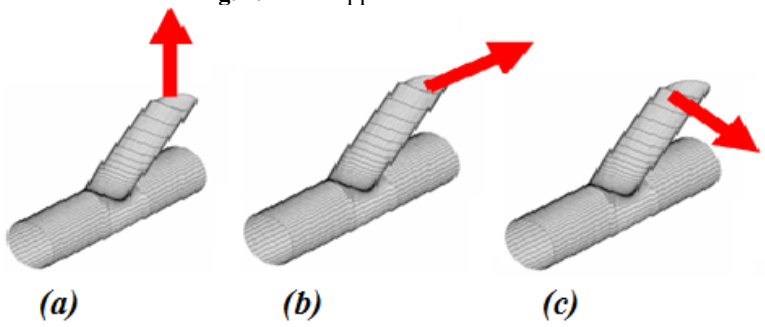

Fig. 5. Loads applied to Y structure.

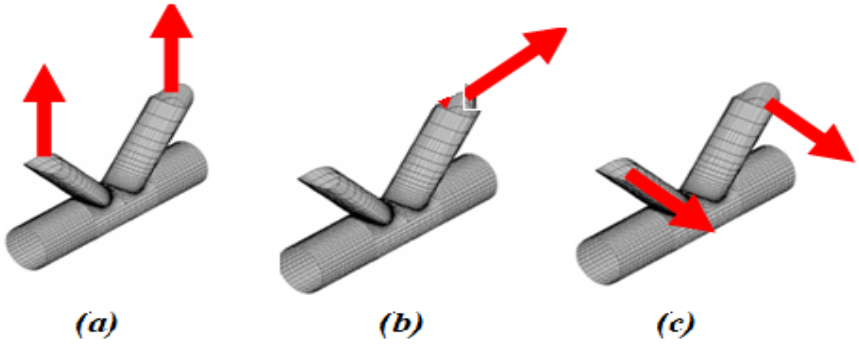

Fig. 6. Loads applied to K structure.

4. Results and discussion

4.1 Axial force

The Von Mises stresses will be calculated at the center of gravity of each of the finite elements, so as to have only an average value of the stress tensor per finite element considered. In Fig. 7, we note that the stress concentration around the junction is distributed symmetrically and these in two points, it is largely visible in the vicinity of the two quarter points which promote the appearance of the hot spot in these two points.

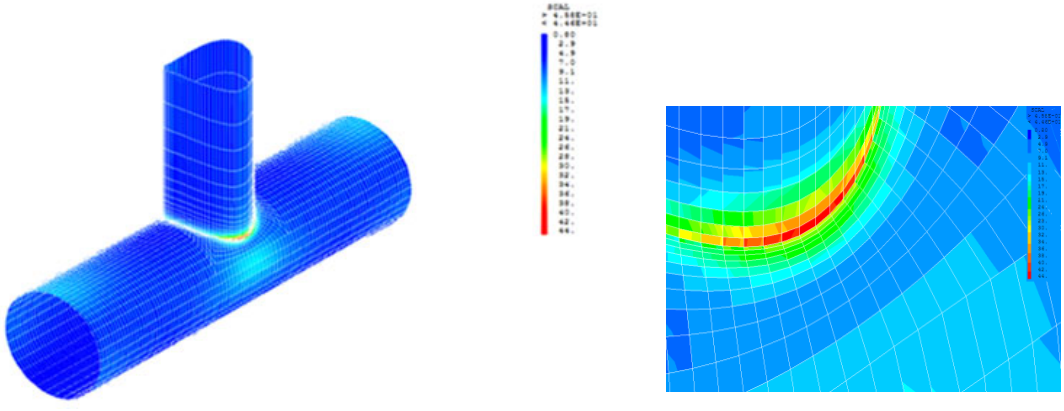

Fig. 7. *(a)* Tensile Stress Concentrations T Structure, *(b)* Zoom of stress concentration zone

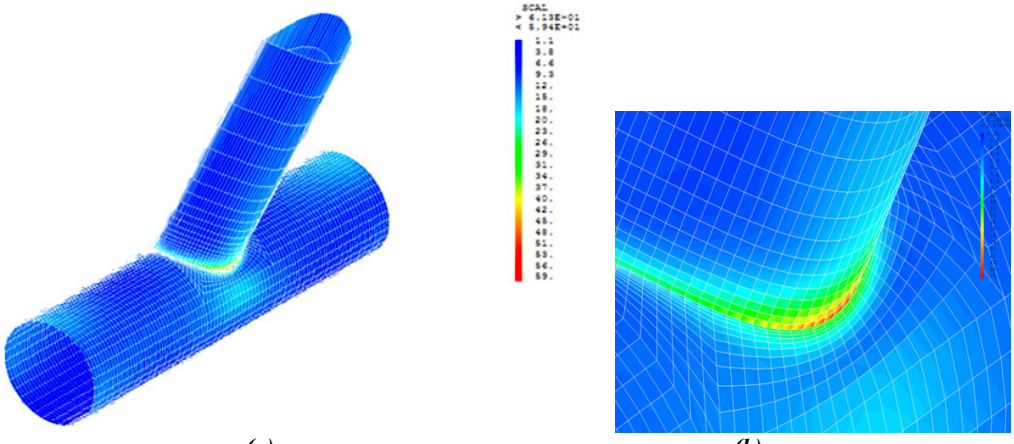

(a) *(b)*

Fig. 8. *(a)* Tensile Stress Concentrations Y Structure, *(b)* Zoom of stress concentration zone.

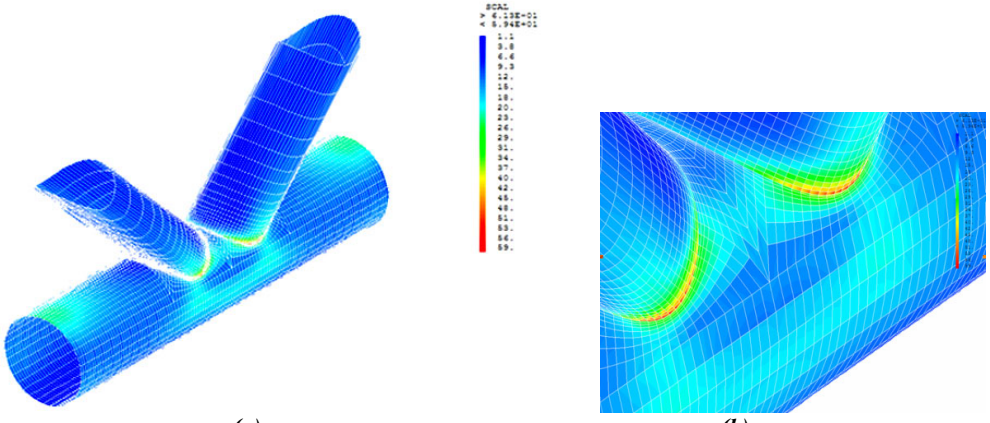

(a) *(b)*

Fig. 9. *(a)* Tensile Stress Concentrations K Structure, *(b)* Zoom of stress concentration zone.

4.2 Axial force Bending out of plan (BOP)

This stress will generate a deformation which will be localized only on the chord (a part undergo a tension and the other a compression). One can distinguish a similarity in the distribution of the stress concentration with the tension that is to say that the concentration is located at the two quarter points (Fig. 10).

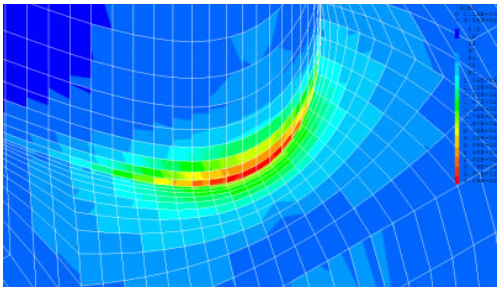

Fig. 10. Out-of-plane bending stress concentrations (T structure).

4.3 In plane bending

In this case, a bending is applied in the direction of the chord, thus creating a deformation made by the compression on one side and the traction on the other. Note that most of the deformation is located on the chord near the junction between the two tubes, the spacer also undergoes deformation but on a smaller scale (Fig. 11).

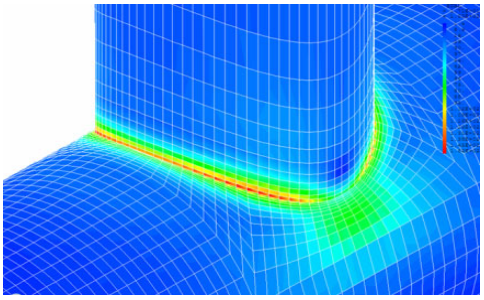

Fig. 11. In-plane bending stress concentration.

Contrary to the two preceding cases of loading, the concentration of the stresses is no longer located very close to the quarter point but it is deviated towards the pommel point. In the two previous cases we distinguish the presence of two hot spots, in the FDP there are four spots, but the symmetry in the distribution of the concentration still exists.

4.4 Calculation of Stress Concentration Factors (K_t)

4.4.1 Simple load

For reasons of symmetry, two quarters of the T structure will be studied, so the study will focus on the portion located between the two pommel points at an angle $\Phi = 0°$ and $\Phi = 180°$. Fig. 12 represents the evolution of the stress concentration factor (K_t) as a function of the positioning angle (Φ_i) between (0° and 180°).

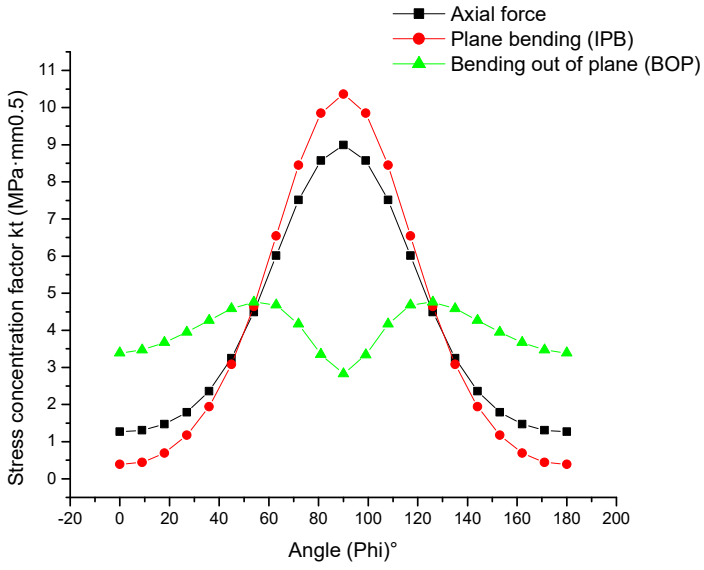

Fig. 12. Curve of variation of K_t according to Φ_i Stress on the structure.

For Axial force, the latter evolves according to the angle (Φ_i) is reached a maximum (K_t=8.99) located at (Φ_i =900) cartier point. For the case of out of Plan Bending, notes that the concentration evolves in the same way as in the case of traction, except that the values are lower than those of traction. The minimum value is always located at the pommel point at an angle and the maximum value at $\Phi_i = 0°$ the quarter point at an angle $\Phi_i = 90°$ (K_t=10.36). It is noted that in the case of the BOP the hot spot has a value greater than that of the traction. For Bending in Plane, the same way as in the case of the two other loadings, the curve representing the evolution of the K_t as a function of Φ_i is drawn, but this time the shape of the curve is totally different from the two others. The stress concentration factor always evolved according to (Φ_i) and this time it presents two peaks: The first peak (K_t=4.77) located at the point (Φ_i =58.50) and the second peak (K_t=4.77) located at the point deviate from the neighborhood point located at (Φ_i =121.50).

The concentration in this case, evolves gradually from the pommel point until reaching a maximum value at an angle and then begins to decrease until the quarter point. We note here that the hot point is no longer located at the quarter point like the other two cases.

4.4.2 Combined Loads

We apply a load combination from a traction and bending out of the plane (BOP) in first, next a load combination from a traction and bending in plane (BIP) with a load ratio equal to one (Tr/BOP=1, Tr/BIP=1 with a load =4MPa). In Fig. 13 the evolution of the stress concentration factor (K_t) as a function of the positioning angle (Φ_i) between (0° and 180°) have represented. In the case of bending out of the plane (BOP), we have observed that the latter evolves as a function of the angle (Φ_i) and grasse than a maximum (K_t=0.88) located at (Φ_i =90°) cartier point. In the case of bending in plane (BIP), we found that the latter evolves according to the angle (Φ_i) and fat that a maximum (K_t= 0.17) located at (Φ_i = 90°) cartier point.

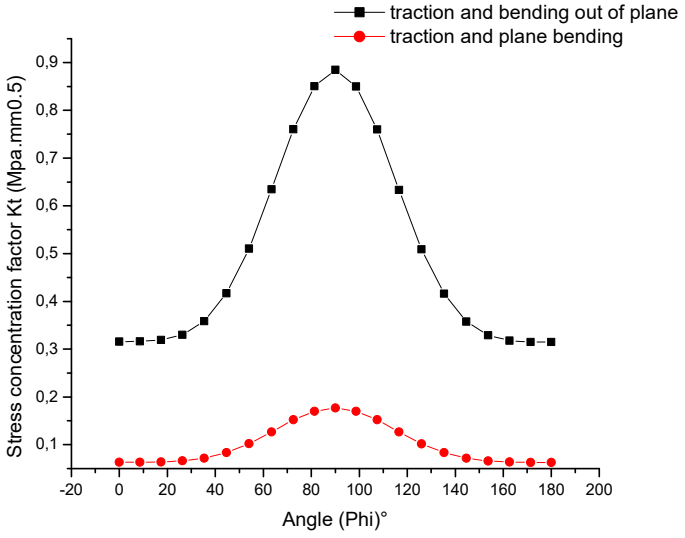

Fig. 13. Curve of variation of K_t according to Φ_i Stress on the structure.

We have represented the curves of (K_t) as a function of the positioning angle (Φi) and those for the aforementioned loads. In Fig. 14 and Fig. 15, we constantans that the pace of the curves of variation of the stress concentration factor according to the angle of positioning (Φi) is similar for the two structures (Y and K) Only the two structures Y and K exhibit 4 peaks.

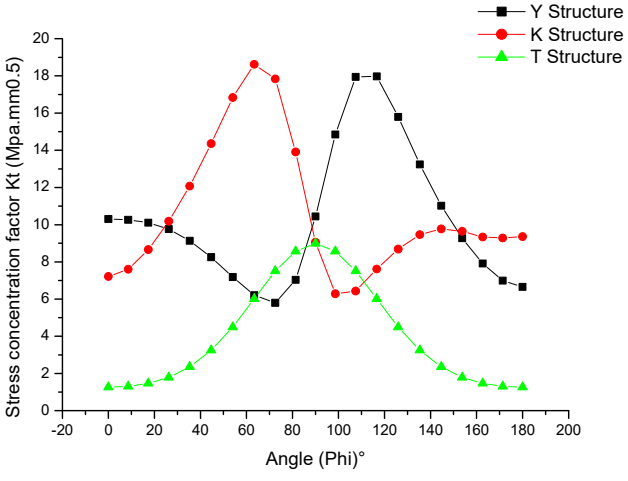

Fig. 14. Comparison of variation curves of $k_t = f(\Phi i)$ of Structures (T, Y and K) under Tensile loading.

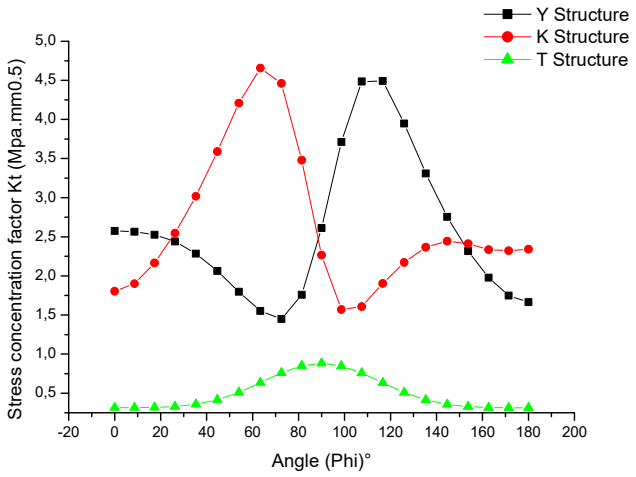

Fig. 15. Comparison of Curves of variation of $k_t = f(\Phi i)$ of Structures (T, Y and K) under combined loading (Tr/Bop).

4.5 Comparison of Results

The values of the stress concentration factor corresponding to the hot spots for the junctions (T, Y and K) are grouped in Table 2; as for the curves of the latter, they are shown in Fig. 10 and Fig. 11.

Table 2. Results obtained by our calculations in the cases of the loadings: Tr, Bop, Bip, and the combinations Tr/Bop, Tr/Bip

Loading	T	Y	K
		k_t	
Tr	k_t =8.99 ; Φ_i=90^0	k_t = 10.31 ; Φ_i=0^0 k_t = 18.34 ; Φ_i=112	k_t = 18.65 ; Φ_i=68^0 k_t = 9.77 ; Φ_i=144.66^0
Bip	k_t =10.36; Φ_i=90^0	k_t = 4.92 ; Φ_i=94.30^0	k_t = 4.16 ; Φ_i=76.98^0 k_t = 5.66 ; Φ_i=180^0
Bop	k_t =4.77; Φ_i=58.5^0 k_t =4.77 ; Φ_i=121.5^0	k_t = 1.98 ; Φ_i=0^0 k_t = 2.62 ; Φ_i=112^0	k_t = 5.08 ; Φ_i=85.70^0
Tr/Bop	k_t = 0.88 ; Φ_i=90^0	k_t = 2.58 ; Φ_i=0^0 k_t = 4.58 ; Φ_i=112^0	k_t = 4.66 ; Φ_i=68^0 k_t = 2.44 ; Φ_i=144.64^0
Tr/Bip	k_t = 0.18 ; Φ_i=90^0	k_t = 0.51 ; Φ_i=0^0 k_t = 0.92 ; Φ_i=112^0	k_t = 0.78 ; Φ_i=68^0 k_t = 0.41 ; Φ_i=144.64^0

Table 3. Comparison of our results with the authors' results

Authors		Kuang et al. (1975)	Gibstein (1978)	N'diaye et al. (2007)	Pang et Lee (1995)	Our Results
Loading				K_t		
Tr	T	9.6	11.2	9.62	/	8.99
	Y	8.3	11.7	9.62	/	18.34
	K	18.8	14.2	13.62	/	18.65
Bop	T	8.6	11.3	10.45	/	10.36
	Y	3.3	4.6	3.11	/	4.92
	K	2.9	4.3	6.45	/	5.66
Bip	T	3.3	3.4	3.11	/	4.77
	Y	2.6	2.3	2.73	/	2.62
	K	3.3	3.4	3.11	/	5.08
Tr/Bop	T	/	/	/	1.17	0.88
	Y	/	/	/	5.1	4.58
	K	/	/	/	4.26	4.66
Tr/Bip	T	/	/	/	1.81	0.18
	Y	/	/	/	0.91	0.92
	K	/	/	/	1.18	0.75

According to the values of Table 2, we note that the stress concentration factor varies according to the geometry of the structure considered, and the loading applied.

From Fig. (14) and Fig. (15), the stress concentration factor curves (for Y and K structures) show some symmetry with respect to the positioning angle with slightly different values, and this for loadings such as: traction, combination (Tr/Bop) and combination (Tr/Bip).

According to Fig. (8) and Fig. (9), structures Y and K present in all loading cases four hot spots located respectively at the points: pommel and/or deviated from the quarter point , except in the case of in-plane bending (for the K-type structure) with two hot spots slightly deviated from the neighborhood point.

In Table 3, we compared the results of the stress concentration factor obtained by our calculations with those of the various authors (Kuang et al., 1975; Gibstein & Moe, 1981; Nazari et al., 2007).

We note that the results obtained by our calculations are closer to those obtained by A. N'diaye, Gibstein and Pang for the T structure and the authors Pang and A. N'diaye for the structures (Y and K).

5. Conclusion

The objective of this study was to determine the stress concentration factors in T, Y and K junctions. Our approach was to use the finite element method with the Castem 2021 software to locate hot spots or areas of high stress concentration stresses, which often constitute sites of initiation and propagation of fatigue cracks, the second objective is to calculate stress concentration factors; this method seems the best suited, because of the complexity and geometric discontinuity of the tubular knots.

This study allowed us to show that the hot spots are generally located at the neighborhood points in the case of the structure (T) for the loadings: tension, bending out of the plane with values of the stress concentration factor which can reach (Tr:8.99, BOP:10.36, BIP:4.77) and which are satisfactory compared to those found by Nazari et al. (2007) (Tr:9.62, BOP:10.45, BIP:3.11). Otherwise at the pommel point and/or deviated from the quarter point in the case of type structures (Y and K) in all loading cases (except the case of in-plane bending for K); our $\boldsymbol{K_t}$ values are close in this case to the values obtained by the authors A. N'diaye and Pang.

The numerical model used has been validated by previous studies devoted to T, Y and K type junctions. These studies have shown that the results obtained are very close to those calculated using the parametric equations of Lloyd and Eftemieux in the case of a tensile stress, bending in and out of the plane. These results are nevertheless slightly higher in practically.

References

Alaoui, A. E. M. (2005). *Influence du chargement sur la propagation en fatigue de fissures courtes dans un acier de construction navale* (Doctoral dissertation, Université de Metz).

Castem software, http://www-cast3m.cea.fr/.

Clough, R. W., & Johnson, C. P. (1968). A finite element approximation for the analysis of thin shells. *International Journal of Solids and Structures*, *4*(1), 43-60.

Efthymiou, M. (1988). Development of SCF formulae and generalised influence functions for use in fatigue analysis.

El Fakkoussi, S., Moustabchir, H., Elkhalfi, A., & Pruncu, C. I. (2019). Computation of the stress intensity factor KI for external longitudinal semi-elliptic cracks in the pipelines by FEM and XFEM methods. *International Journal on Interactive Design and Manufacturing (IJIDeM)*, *13*(2), 545-555.

Fuštar, B., Lukačević, I., & Dujmović, D. (2018). Review of fatigue assessment methods for welded steel structures. *Advances in Civil Engineering*, *2018*.

Gibstein, M. B. (1978, November). Parametric stress analysis of T joints. In *European Offshore Steels Research Seminar[Proc. Conf.]*.

Gibstein, M. B., & Moe, E. T. (1981, October). Numerical and experimental stress analysis of tubular joints with inclined braces. In *SIMS* (Vol. 6, p. 15).

Guidance on Design, "Construction and Certification. HSE". February (1995).

Jukić, K., Perić, M., Tonković, Z., Skozrit, I., & Jarak, T. (2021). Numerical Calculation of Stress Intensity Factors for Semi-Elliptical Surface Cracks in Buried-Arc Welded Thick Plates. *Metals*, *11*(11), 1809.

Karamanos, S. A., Romeijn, A., & Wardenier, J. (2000). Stress concentrations in tubular gap K-joints: mechanics and fatigue design. *Engineering Structures*, *22*(1), 4-14.

Kuang, J. G., Potvin, A. B., & Leick, R. D. (1975). Stress Concentration in Tubular Joints', OTC 2205. *Annual Offshore Technology Confer-ence, May 1975*.

Li, Y., Chen, J., & Ren, N. (2014). Refined fatigue analysis for the tripod support structure of offshore wind turbine (OWT). *EJGE*, *19*, 4193-4200.

Mansouri, K., Abboudi, A., & Djebaili, H. (2022). Vickers Hardness Test of Steel Pipes Welded by High Frequency Induction. *Journal Of Nano- And Electronic Physics. 14* (1).

Nazari, A., Daniel, W. T., Guan, Z., & Gurgenci, H. (2007). Parametric equations using generic representation of joint stiffness. *Journal of Offshore Mechanics and Arctic Engineering, 129*(2), 131-137.

N'diaye, A., Hariri, S., Pluvinage, G., & Azari, Z. (2007). Stress concentration factor analysis for notched welded tubular T-joints. *International Journal of Fatigue*, *29*(8), 1554-1570.

OH, C. Y., Kim, Y. J., OH, Y. J., Song, T. K., & Kim, Y. B. (2012). Estimation of stress intensity factors for circumferential cracked pipes under welding residual stress filed. *Transactions of the Korean Nuclear Society Autumn Meeting*, Gyeongju, Korea.

Pang, H. L. J., & Lee, C. W. (1995). Three-dimensional finite element analysis of a tubular T-joint under combined axial and bending loading. *International journal of fatigue*, *17*(5), 313-320.

PD6493, B. S. I. (1991). Guidance on methods for assessing the acceptability of flaws in fusion welded structures. *British Standard Institute*.

Potvin, A. B., Kuang, J. G., Leick, R. D., & Kahlich, J. L. (1977). Stress concentration in tubular joints. *Society of Petroleum Engineers Journal*, *17*(04), 287-299.

Smedley, S., & Fischer, P. J. (1991, August). Stress concentration factors for ring-stiffened tubular joints. In *First International Offshore and Polar Engineering Conference (ISOPE), Edinburgh, Scotland, Aug* (pp. 11-16).

Wang, X., & Lambert, S. B. (2003). On the calculation of stress intensity factors for surface cracks in welded pipe–plate and tubular joints. *International journal of fatigue*, *25*(1), 89-96.

Wang, H. (2016). Numerical investigation of fracture spacing and sequencing effects on multiple hydraulic fracture interference and coalescence in brittle and ductile reservoir rocks. *Engineering Fracture Mechanics*, *157*, 107-124.

Yao, X. M., Zhang, Y. C., Pei, Q., Jin, L. Z., Ma, T. H., He, X. H., & Zhou, C. Y. (2022). Empirical Solution of Stress Intensity Factors for the Inclined Inner Surface Crack of Pipe under External Pressure and Axial Compression. *Materials*, *16*(1), 364.

Yearbook, S. S. (2017). World Steel Association: Brussels.

Zhen, C. H. E. N., Xue-Qing, L. I. U., Kui, W. A. N. G., Lu-Yi, L. U., & Qing-Ren, W. A. N. G. (2016, December). Cracking failure analysis of T-type welded tee in waste heat boiler. In *3rd International Conference on Material Engineering and Application (ICMEA 2016)* (pp. 427-432). Atlantis Press.